Circularly polarized zero-phonon transitions of vacancies in diamond at high magnetic fields

D. Braukmann,[1] E. R. Glaser,[2] T. A. Kennedy,[2] M. Bayer,[1,3] and J. Debus[1,*]
[1]*Experimentelle Physik 2, Technische Universität Dortmund, 44227 Dortmund, Germany*
[2]*Naval Research Laboratory, Washington, DC 20375, USA*
[3]*Ioffe Institute, Russian Academy of Sciences, 194021 St. Petersburg, Russia*

(Received 18 March 2018; published 29 May 2018)

We study the circularly polarized photoluminescence of negatively charged (NV^-) and neutral (NV^0) nitrogen-vacancy ensembles and neutral vacancies (V^0) in diamond crystals exposed to magnetic fields of up to 10 T. We determine the orbital and spin Zeeman splitting as well as the energetic ordering of their ground and first-excited states. The spin-triplet and -singlet states of the NV^- are described by an orbital Zeeman splitting of about 9 μeV/T, which corresponds to a positive orbital g-factor of $g_L = 0.164$ under application of the magnetic field along the (001) and (111) crystallographic directions, respectively. The zero-phonon line (ZPL) of the NV^- singlet is defined as a transition from the $^1E'$ states, which are split by $g_L\mu_B B$, to the $^1A_1$ state. The energies of the zero-phonon triplet transitions show a quadratic dependence on intermediate magnetic field strengths, which we attribute to a mixing of excited states with nonzero orbital angular momentum. Moreover, we identify slightly different spin Zeeman splittings in the ground (gs) and excited (es) triplet states, which can be expressed by a deviation between their spin g-factors: $g_{S,\mathrm{es}} = g_{S,\mathrm{gs}} + \Delta g$ with values of $\Delta g = 0.014$ and 0.029 in the (001) and (111) geometries, respectively. The degree of circular polarization of the NV^- ZPLs depends significantly on the temperature, which is explained by an efficient spin-orbit coupling of the excited states mediated through acoustic phonons. We further demonstrate that the sign of the circular polarization degree is switched under rotation of the diamond crystal. A weak Zeeman splitting similar to $\Delta g\mu_B B$ measured for the NV^- ZPLs is also obtained for the NV^0 zero-phonon lines, from which we conclude that the ground state is composed of two optically active states with compensated orbital contributions and opposite spin-1/2 momentum projections. The zero-phonon lines of the V^0 show Zeeman splittings and degrees of the circular polarization with opposite signs. The magnetophotoluminescence data indicate that the electron transition from the $^1T_2$ states to the ^1A ground state defines the zero-phonon emission at 1.674 eV, while the $^1T_2 \rightarrow {}^1E$ transition is responsible for the zero-phonon line at 1.666 eV. The $^1T_2$ (^1E) states are characterized by an orbital Zeeman splitting with $g_L = 0.071$ (0.128).

DOI: 10.1103/PhysRevB.97.195448

I. INTRODUCTION

The neutral and negatively charged nitrogen-vacancy centers in diamond have been studied in recent years on account of possible applications in quantum information processing, spin electronics, quantum sensing, and biophotonics [1–3]. Particular focus has been drawn to their optical properties. For negatively charged nitrogen vacancies (NV^-), the ground state forms a two-level quantum system thus serving as a quantum bit, whose state can be controlled coherently by electron spin resonance [4]. The coherent manipulation of a single electron spin quantum-bit associated with an NV^- center could, for example, be exploited to detect very weak magnetic fields [5], while fluorescent nanodiamonds inside living cells could create new possibilities for quantum-based imaging in life sciences [6].

In general, the NV center consists of a substitutional nitrogen atom, which is paired with a vacancy in the diamond lattice. The NV^- center embraces six electrons that are localized at the vacancy [7]. The ground and first-excited states of the NV^- center are spin-triplet states. The optical transition between excited and ground states is a pure electronic transition without phonon support; accordingly, it is denoted as a zero-phonon line (ZPL) and, for the NV^-, it has an energy of about 1.946 eV. In the case of a localization of five electrons at the vacancy the nitrogen-vacancy center is neutral (NV^0). Its ground and excited states are spin-doublet states yielding a ZPL at about 2.156 eV [8,9]. When only a vacancy without association to a nitrogen atom is present in the diamond lattice, a neutral vacancy V^0 can be formed. It exhibits two ZPLs at about 1.665 and 1.673 eV [10].

Although considerable achievements in different fields of fundamental research and applications have been obtained, optical properties of the nitrogen vacancies and neutral vacancy in diamond in the presence of large magnetic fields, which exceed hundreds of milliteslas typically applied in electron-spin resonance experiments, have rarely been studied. A single spectrum of the NV^- singlet-state ZPL at 1042 nm (1.19 eV) was measured at 5 T [11], the temperature dependence of an effective orbital g-factor was studied at 5 T through magnetic circular dichroism [12], and the Zeeman splitting of the left- and right-handed circularly polarized NV^- triplet-state ZPL was measured up to magnetic fields of 150 T at 77 K, from which an orbital g-factor of 0.22 was evaluated [13]. Recently the linear polarization properties of the NV^-, NV^0, and V^0

*Corresponding author: joerg.debus@tu-dortmund.de

ZPLs up to 10 T were investigated [14]. Nevertheless, studies of magneto-optical effects for the NV^- and, in particular, for the NV^0 and V^0 in diamond at high magnetic fields are underrepresented. Such studies may provide considerable insight into the fine structure of the vacancies and spin-based interactions as well as magnetic-field-induced changes of, for example, linear and nonlinear optical responses of the vacancies in diamond. The fine structure defines the optical and electronic properties of solid-state materials and its knowledge plays a major role in applying magnetic resonance techniques as well as in realizing optoelectronic devices, in which, for example, carrier inter- and intraband relaxation processes affect the optical quantum yield. In the context of determining the fine structures, the orderings of the singlet NV^- states and ground states of the neutral vacancy are still under debate. For the NV^- spin-singlet states, the ZPL emission was attributed to an $^1A_1 \rightarrow {}^1E$ transition [15], while in Ref. [16] it was related to the $^1E' \rightarrow {}^1A_1$ transition. Revealing the level ordering of the singlet states is important for describing the photostability of NV^- centers and their emission efficiency, which depends on the triplet-singlet intersystem crossing [17]. For the V^0, it was proposed that the ZPL at 1.673 eV is related to the transition from the $^1T_2$ to the ^1E states and the ZPL at 1.665 eV should correspond to a transition from the $^1T_2$ to the ^1A state [10,18]. It was further indicated that the V^0 luminescence is unpolarized, even in the case of polarized exciting light [19], and that the orbital g-factor is negligibly small [20].

In this paper, we report on the orbital and spin Zeeman splittings and circular polarization characteristics of the zero-phonon lines of ensembles of the negatively charged and neutral nitrogen vacancies as well as the neutral vacancy in diamond crystals under application of high magnetic fields up to 10 T. The orbital Zeeman splitting of the triplet-state transitions of the NV^- centers coincides with that of the singlet-state transitions, while the ZPL of the NV^0 centers shows a negligible magnetic-field-dependent splitting. Hereby, we determine that the singlet-state transitions of the NV^- go from the $^1E'$ states, whose splitting is proportional to $g_L = 0.164$, to the $^1A_1$ ground state. For the two ZPLs of the V^0 at about 1.666 and 1.674 eV, the Zeeman splittings have opposite signs and different absolute values indicating different orbital Zeeman contributions of the $^1T_2$ and ^1E states. We attribute the ZPL at 1.674 eV to the $^1T_2 \rightarrow {}^1A_1$ transition and the ZPL at 1.666 eV to the $^1T_2 \rightarrow {}^1E$ transition. We observe a quadratic evolution of the triplet NV^- ZPL energy with increasing magnetic field. We propose that it results from a mixing of excited states with a nonzero orbital quantum number. Moreover, slightly different spin splittings in the ground and excited triplet states are evaluated from the energies of the ZPLs having the same circular polarization under optical excitation with opposite circular polarizations. The circular polarization degree of the NV^- ZPLs depends significantly on the temperature, which is attributed to an efficient spin-orbit coupling of the excited states mediated through acoustic phonons. We further demonstrate that the sign of the circular polarization degree is switched under rotation of the diamond crystal. Also, the circular polarization degree is enhanced by about 10% through excitation with laser light that is linearly polarized along the (001) NV^- center axis.

The paper is organized as follows: In Sec. II, the diamond crystal samples and the experimental setup are described. In Sec. III, the magnetic field dependence of the ZPL energies of the NV^-, NV^0, and V^0 for different circular polarization configurations are shown. Moreover, the magnetic-field-induced degrees of the circular polarization as well as the dependence of the circular polarization degree on the crystal orientation and on the sample temperature are presented. In Sec. IV, the fine structures of the different vacancies are discussed with respect to the magneto-optical results, and reasons for the impacts on the degrees of the circular polarization are described.

II. EXPERIMENTAL DETAILS

We studied a transparent rose-cut diamond crystal grown by chemical vapor deposition with an NV center concentration of about 0.14 ppm (2.5×10^{16} cm^{-3}), denoted as sample 1, and a yellow rectangular-prism-shaped diamond crystal, sample 2, which had an NV center concentration of about 2.9 ppm (5.1×10^{17} cm^{-3}). The latter was grown by high-temperature high-pressure synthesis, electron-irradiated at an energy of 2 MeV, and subsequently annealed [21]. The rose-cut diamond was optically addressable along the (001) direction, while the rectangular-prism-shaped diamond was excited along the (111) direction.

In the optical measurements the diamond crystals, stress-free mounted on a rotation holder inside a variable-temperature insert of a split-coil cryostat, were exposed to helium gas allowing for temperature variations between 6 and 300 K and to magnetic fields ranging from -10 to $+10$ T. The magnetic field **B** was applied along the aforementioned optically accessible axes of the crystals. The error in aligning the crystal axes with respect to the magnetic field direction was about $\pm 1^\circ$. The crystal surfaces were masked by a black polycarbonate layer with a hole of 0.5 mm diameter for the laser excitation. The illumination of a sample was checked by an intermediate image using a cross slit and microscope. Typically, the laser spot diameter was 400 μm and by use of the cross slit its central part with an area of about $100 \times 100\ \mu$m^2 was selected. For the excitation of the vacancies, either a diode-pumped solid-state laser (Coherent Verdi V10) with an emission energy of $E_{\text{exc}} = 2.33$ eV or a continuous-wave single-frequency ring dye laser (Coherent 899-29) equipped with Rhodamine 6G, $E_{\text{exc}} = (1.95 - 2.23)$ eV, was used. In both cases the power density of the laser spot at the sample surface was kept at about 25 mW/cm^2 using a variable neutral-density filter. Any fluctuations in the laser power were permanently monitored and were considered in the intensity normalization of the photoluminescence (PL) spectra. A notch-filter, which was installed after the dye-laser output mirror, suppressed the pump-laser beam (2.33 eV), thus avoiding any additional excitation of the vacancies.

The circular (linear) polarization of the laser beam was controlled by a Glan-Thompson prism followed by an achromatic quarter-wave (half-wave) retarder plate. The circularly polarized emission from the vacancies was in turn analyzed by an achromatic quarter-wave plate and a linear polarizer. Finally, the emission was dispersed by a triple monochromator working in the additive mode with a total focal length of 1.5 m and was detected by a liquid-nitrogen-cooled silicon charged-coupled

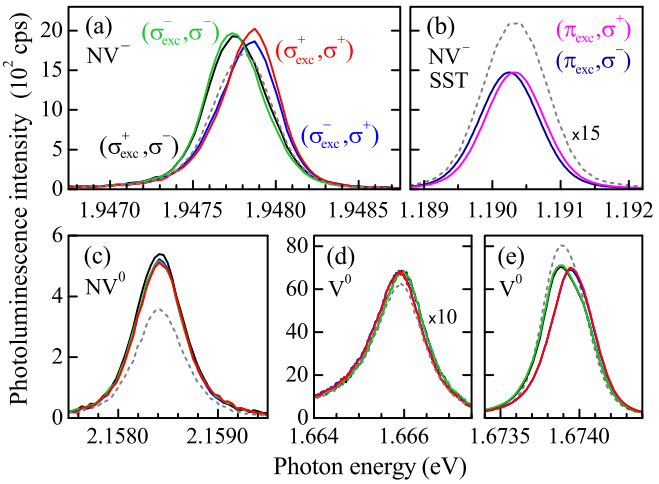

FIG. 1. PL spectra measured in different polarization configurations at 10 T (solid lines) and 0 T (dashed lines) for the (a) NV^- triplet transitions, (b) NV^- singlet transition, (c) NV^0 ZPL, and (d, e) V^0 ZPLs. The exciting laser light ($E_{exc} = 2.33$ eV) and magnetic field were directed along the (001) axis of the rose-cut diamond crystal, sample 1. Note that the scaling of the x axis is different in each panel.

device (CCD) camera [22]. The spectral resolution of the monochromator was about 20 μeV. The singlet transition of the NV^- centers, whose emission lies in the infrared spectral range at 1.19 eV, was detected by a liquid-nitrogen-cooled InGaAs CCD camera.

The circular polarization degree of the PL emission, which is given by the third Stokes parameter [23], is defined by

$$\rho_c^{\pi} = \frac{I_+^{\pi_{exc}} - I_-^{\pi_{exc}}}{I_+^{\pi_{exc}} + I_-^{\pi_{exc}}}. \quad (1)$$

Here, $I_{+(-)}$ is the intensity of the $\sigma^{+(-)}$-polarized PL under linearly polarized excitation, which is marked by the upper index. For the magnetic-field-induced circular polarization degree, we alternatively use the definition

$$\rho_c^{\sigma} = \frac{\rho_c^{\sigma,+} + \rho_c^{\sigma,-}}{2} = \frac{1}{2}\left(\frac{I_+^+ - I_-^+}{I_+^+ + I_-^+} + \frac{I_+^- - I_-^-}{I_+^- + I_-^-}\right), \quad (2)$$

which represents the mean value of the circular polarization degrees obtained for both circularly polarized excitations [24]. In the following the circular polarization configurations are indicated by the notation $(\sigma_{exc}^{\eta},\sigma^{\gamma})$, where σ_{exc}^{η} and σ^{γ} designate the circular polarizations of the exciting and detected light, respectively. The sign of η and γ is determined by the sign of the photon angular momentum projection on the optical axis.

III. RESULTS

The PL spectra of the oppositely circular-polarized zero-phonon transitions of the negatively charged and neutral nitrogen vacancies as well as neutral vacancy are shown by the solid lines in Fig. 1 measured at a temperature of 6 K. The strength of the magnetic field is $B = 10$ T and its direction is along the (001) axis of the rose-cut diamond crystal. By comparison, nonpolarized spectra recorded at zero magnetic field are depicted by the gray dashed lines.

The zero-phonon lines of the NV^- ensemble are shown for the four different circular polarization configurations in Fig. 1(a). The σ^+-polarized ZPLs (red and blue lines) are shifted to higher energies, while the σ^--polarized ZPLs (black and green lines) are shifted to lower energies in comparison to the ZPL energy of $E_{ZPL}(B = 0\text{T}) = E_{ZPL}(0) = 1.94780$ eV obtained at 0 T. The energy shifts amount to about +50 and −35 μeV, respectively. The singlet state transitions (SSTs) of the NV^- show a similar behavior; the energy difference between the oppositely polarized lines is about 80 μeV [see Fig. 1(b)] [25]. In contrast to the NV^- related lines, the ZPL of the NV^0 does not split significantly in a magnetic field of 10 T for any of the polarization configurations, as depicted in Fig. 1(c); the ZPL peak energy remains at 2.15842 eV. Besides the NV centers, the zero-phonon transitions of the V^0 demonstrate notable Zeeman shifts, as one can see in Figs. 1(d) and 1(e) for its low-energy ZPL at 1.66586 eV and its high-energy one at 1.67390 eV. For the latter ZPL, we observe an energy shift to high (low) energies in the σ^+ (σ^-) polarization. The low-energy ZPL, however, shows an opposite magnetic field dependence, where the σ^+-polarized (σ^--polarized) lines are shifted to low (high) energies. Note that the line shapes can be best described with Voigt functions with approximately equal Gaussian and Lorentzian contributions. The low-energy V^0 ZPL has a low-energy flank making the line shape asymmetric. With increasing magnetic field the line profiles do not change significantly.

To gain further insight into the magnetic field dependencies of the circularly polarized zero-phonon transitions, we study the Zeeman splitting of the oppositely polarized ZPLs under, in most cases, circularly polarized excitation. We define the Zeeman splitting as the difference between the energies $E_{ZPL,+}$ and $E_{ZPL,-}$ of the right- and left-handed circular-polarized ZPLs: $\Delta E_Z = E_{ZPL,+} - E_{ZPL,-}$. As one can see in Fig. 2(a), the Zeeman splitting of the NV^- spin-triplet ZPLs, for sample 1 in the (001) geometry, evolves linearly and is inversely symmetric around $B = 0$ T; a zero-field splitting is negligible. At $B = +9$ T, $\Delta E_Z = (87 \pm 2)$ μeV and, at $B = -9$ T, $\Delta E_Z = (-84 \pm 2)$ μeV, for both circular excitation polarizations. Thus, the oppositely circular-polarized NV^- ZPLs are split in an external magnetic field by about 9.5 μeV/T. A comparable Zeeman splitting of about 9.1 μeV/T is obtained for the SSTs of the NV^- centers, as shown for linearly polarized excitation in Fig. 2(b). In contrast to that, the NV^0 ZPL does not show a significant splitting with rising magnetic field [see Fig. 2(c)]. A weak splitting of 1.2 (0.7) μeV/T, for σ_{exc}^+- (σ_{exc}^--)polarized laser light, can be deduced from the experimental data.

The Zeeman splitting of the low-energy V^0 ZPL is depicted in Fig. 2(d), while in Fig. 2(e) ΔE_Z of the high-energy V^0 ZPL is shown. In both cases, the Zeeman splitting tends to zero at 0 T; i.e., a zero-field offset is negligible and the opposite excitation polarizations result in similar $\Delta E_Z(B)$ dependencies. A notable discrepancy, however, shows up in opposite and different gradients of the Zeeman splittings of −7.4 and +4.1 μeV/T for the low- and high-energy ZPL, respectively. Note that the $\Delta E_Z(B)$ dependence of the high-energy ZPL could be described as slightly asymmetric around 0 T, which can result from a weak negative zero-field offset of −5 μeV. A significant asymmetry is seen for the $\Delta E_Z(B)$

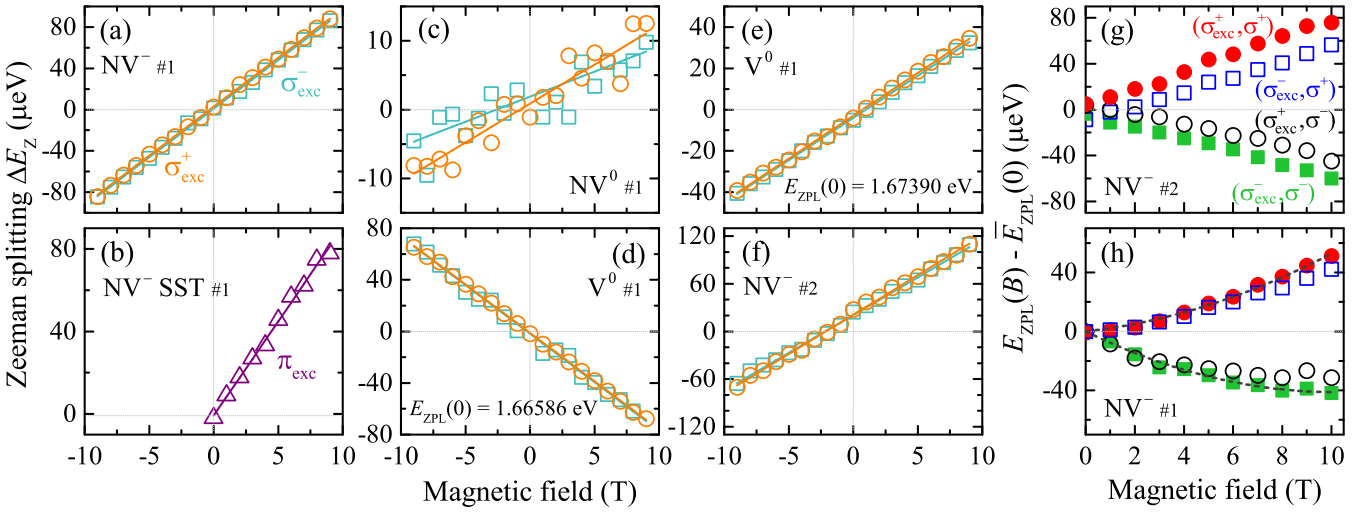

FIG. 2. Zeeman splitting of the ZPLs emitted by the (a, b) NV^- and (c) NV^0 centers as well as the (d, e) neutral vacancies, for sample 1 in (001) geometry, and by the (f) NV^- centers, for sample 2 in (111) geometry, measured at σ^+_{exc} (open circles) and σ^-_{exc} (open squares) or π_{exc} (open triangles) polarized excitation; $T = 6$ K, $E_{exc} = 2.33$ eV. The solid lines are fits according to Eq. (4). The difference between the ZPL energies $E_{ZPL}(B)$ with respect to the averaged zero-field value $\bar{E}_{ZPL}(0)$ for the NV^- centers of (g) sample 2 and (h) sample 1; $T = 6$ K, $E_{exc} = 2.20$ eV. The fits of the data points, for the co-circularly polarized configurations, are shown by the dashed lines in (h); the fits are based on the equation $\alpha B^2 + \beta B$. The error does not exceed the symbol size.

dependence of the NV^- centers, for sample 2, as is shown in Fig. 2(f). It is due to a large zero-field offset of $\delta = +21$ μeV. The Zeeman splitting is given by 9.7 μeV/T for both circular excitation polarizations, which practically coincides with the splittings obtained for the NV^- centers' ZPLs in sample 1.

The afore-described Zeeman splitting does not indicate changes, which affect in the same manner the energies of the circularly polarized transitions. Therefore, we now take a look at changes in the absolute energies of the ZPLs with respect to the averaged value of their zero-field energies; in particular, for the NV^- centers we obtain peculiarities. For sample 2 at strong magnetic fields, see Fig. 2(g), one spectrally distinguishes four NV^- ZPL peaks according to the different circular polarization configurations. For a specific circular polarization in the detection, the switching of the excitation polarization yields two peak energies differing by (19 ± 5) μeV from each other (see red and blue as well as black and green symbols). At zero field the peak energies, for the co-circular polarization configurations, demonstrate a difference of at most 15 μeV, which nearly agrees with the offset evaluated from the $\Delta E_Z(B)$ dependence shown in Fig. 2(f). One may also identify a weak nonlinearity in the magnetic field dependence of the σ^--polarized ZPL energies (black and green symbols). Clearly visible is a nonlinear evolution of the ZPL energies for sample 1, as shown in Fig. 2(h). Using a parabolic αB^2 combined with a linear βB magnetic field dependence the fitting of the data points yields $\alpha = (0.4 \pm 0.1)$ μeV/T^2, and $\beta = 1.7(-8.1)$ μeV/T for the σ^+-polarized (σ^--polarized) ZPLs. The convex parabolic curvature can be modeled only by a positive proportionality factor α; thus, the linear contributions differ in their signs and magnitudes. Besides that, since the parabolic curvatures are similar, they cancel each other out in the Zeeman splitting determination. It is further worthwhile to mention that a zero-field offset for sample 1 is negligibly small; it is less than 5 μeV.

In the following the circular polarization degrees of the vacancies' ZPLs are described. In Fig. 3(a) the circular polarization degree ρ_c^π under linearly polarized excitation, according to Eq. (1), is shown for magnetic field strengths varying between -9 and $+9$ T. For the NV^- in sample 2 (light blue pentagons) and high-energy-V^0 ZPL in sample 1 (black triangles), one observes that the $\rho_c^\pi(B)$ dependencies are symmetric around 0 T, which have maximum positive values of about $+4\%$ at negative fields and minimum values of about -3% at positive fields. By comparison, the circular polarization degrees, for the NV^- (green dots) and NV^0 (red squares) in sample 1, deviate significantly from zero in the absence of an external magnetic field taking values of -5% and -8%, respectively. Their linear field dependencies tend to zero at -9 T and have slopes of about -0.6%/T and -0.7%/T, respectively. Moreover, in Fig. 3(c), ρ_c^π is depicted for the low-energy-V^0 ZPL and singlet-state transition of the NV^- measured in sample 1. Both evolutions do not differ significantly from 0% in the whole magnetic field range from -9 to $+9$ T. One can attribute a weak positive slope to the dependence of the circular polarization degree of the V^0 ZPL.

The circular polarization degree ρ_c^σ under circularly polarized excitation, determined by Eq. (2), is shown as a function of the magnetic field in Fig. 3(b). The dependencies for the NV^- in sample 2 and V^0 in sample 1 are quite similar to their $\rho_c^\pi(B)$ evolutions. The main difference is their deviation from zero at 0 T by $+2\%$ and $+4\%$, respectively. ρ_c^σ, for the NV^0 in sample 1, does not show any strong changes with magnetic field staying at about $+2\%$ (see open squares), which is in contrast to the respective ρ_c^π values. In the case of the NV^- centers in sample 1, ρ_c^σ also remains at $+2\%$ for $B \leqslant 0$ T and decreases slightly with rising positive magnetic fields.

In Fig. 4(a) the circular polarization degree ρ_c^π is shown as a function of the sample rotation angle around the (001) axis of sample 1. The exciting laser light is linearly polarized

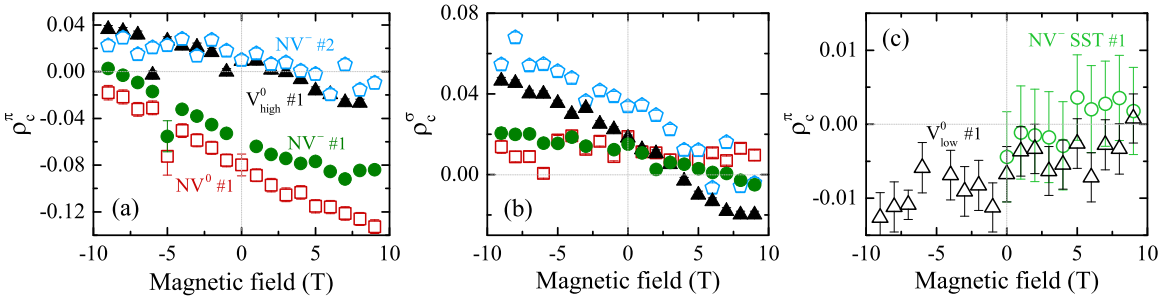

FIG. 3. Magnetic field dependencies of the circular polarization degrees (a) ρ_c^π and (b) ρ_c^σ for the NV^-, NV^0, and high-energy-V^0 ZPLs measured in the (001), sample 1, or (111), sample 2, geometry; $T = 6$ K, $E_{exc} = 2.33$ eV. (c) ρ_c^π for the NV^- SST and low-energy-V^0 ZPL in sample 1, (001) direction. Unless shown otherwise, the experimental error does not exceed the symbol size.

perpendicular to the (001) direction. At 0 T the angular dependence demonstrates a variation between $\rho_c^\pi = +0.1$ and -0.1 with a periodicity of 180°. A fit with a sine function according to $\rho_c^\pi(\phi) = A\sin(2\phi + \phi_0) + b$ with an amplitude $A = 0.088 \pm 0.004$, a phase angle $\phi_0 = (90 \pm 1)°$, and an offset $b = 0.016 \pm 0.003$ describes the data well (see black curve). The presence of an external magnetic field of $B = 6$ T along the (001) direction only weakly affects the amplitude $A = 0.075 \pm 0.005$ and offset $b = 0.011 \pm 0.004$ of $\rho_c^\pi(\phi)$ (see the green-colored dots and curve). However, a remarkable shift in the phase, $\phi_0 = (79 \pm 2)°$, is observed. The latter indicates a magnetic-field-induced phase shift of $\Delta\phi_0 = (11 \pm 2)°$.

In Fig. 4(b) the temperature dependence of the circular polarization degree is shown exemplarily for the NV^- centers measured in sample 2 in the (111) geometry at $B = -10$ T. The circular polarization degree under circularly polarized excitations decreases from -6% between 1.8 and 10 K to about -2% at 250 K. Here, the sign of ρ_c^σ is opposite to that of the values shown in Fig. 3(b), which is due to different in-plane rotation angles of the diamond crystal used in the measurements. The evolution of $\rho_c^\sigma(T)$ can be modeled by a polynomial function of third order ($\propto T^3$) (see light blue curve). It is worthwhile to mention that the circular polarization degrees of the NV^- and NV^0 ZPLs, for sample 1 in the (001) geometry, demonstrate similar temperature dependencies. The V^0 ZPLs lose their circular polarization degrees more rapidly with rising temperature; in the inset of Fig. 4(b) the respective ZPLs measured at different temperatures are shown. The ZPLs strongly broaden with increasing temperature; from 6 to 140 K the linewidths of the ZPLs enhance by more than one order of magnitude.

The dependence of the circular polarization degree ρ_c^σ on the excitation energy is presented in Fig. 4(c), for $B = -9$ T and $T = 6$ K. ρ_c^σ remains at about -6%, for tuning the excitation energy between 1.95 and 2.22 eV. Thus, the variation in the excitation energy has a negligible impact on the circular polarization degree. Note that the degree of the circular polarization does also not depend on the laser power (not shown here).

IV. DISCUSSION

Let us start with the description of the known spin-triplet structure of the negatively charged nitrogen vacancy. We further discuss the changes in the energies of the NV^- ZPLs induced by high external magnetic fields. Afterwards, we extend the discussion to the NV^0 and V^0 in order to characterize their fine structures and circular polarization features.

A. Negatively charged nitrogen-vacancy centers, NV^-

An NV^- center consists of a substitutional nitrogen atom associated with a vacancy in an adjacent lattice site possessing

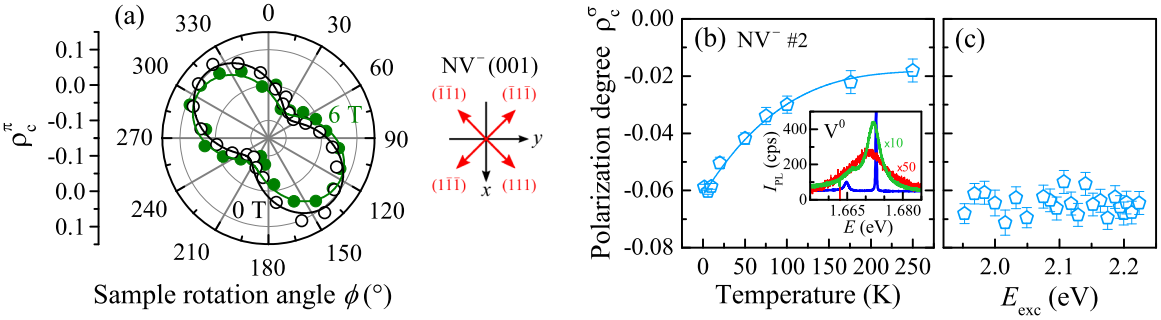

FIG. 4. (a) Angular dependence of the degree of the NV^- ZPL circular polarization, ρ_c^π, at $B = 0$ T (open circles) and 6 T (green dots) in (001) geometry, sample 1; $T = 6$ K. The solid lines are fits based on a sine function. The experimental error does not exceed the symbol size. The orientation of the NV center axes (red arrows) is shown in the panel on the right-hand side. (b) Temperature dependence of the circular polarization degree ρ_c^σ for the NV^- ZPL in sample 2, (111) geometry; $B = -10$ T. The solid line is a third-order polynomial fit. Inset: PL spectra of the V^0 ZPLs at 6 K (blue curve), 140 K (green curve), and 290 K (red curve); $B = 0$ T. (c) Excitation energy dependence of ρ_c^σ for the NV^- in sample 2; $B = -9$ T, $T = 6$ K.

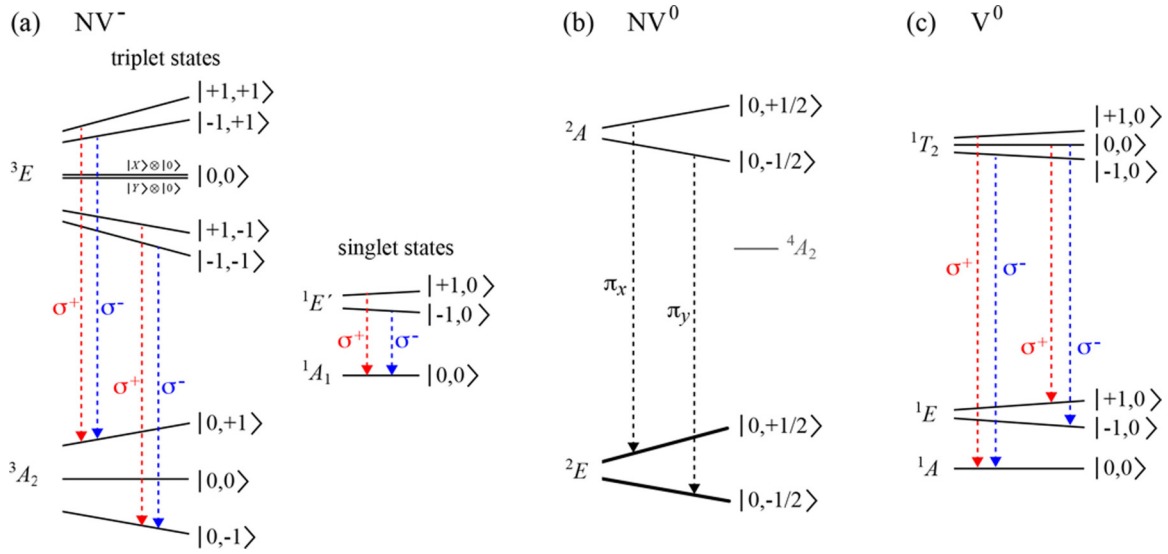

FIG. 5. Level structure schemes of the (a) NV^-, (b) NV^0, and (c) V^0 at high magnetic fields, when the Zeeman energies exceed other intraband splittings, which is approximately the case for $B > 3$ T. The states are denoted by the orbital and spin momentum projections following the notation $|m_L,m_S\rangle$. Zero-phonon transitions are indicated with single-arrowed dashed lines; dashed red and blue lines indicate σ^+-polarized and σ^--polarized transitions, respectively; dashed black lines mark linearly polarized transitions.

C_{3v} symmetry. The six localized electrons of the NV^- center form a discrete level structure [26]. Four of the six electrons are distributed over the defect level a_1 as well as the p-like orbitals e_x and e_y, whose energies lie within the diamond band gap. The lowest occupation of these orbitals defines the spin-triplet ground state $^3A_2$, which is characterized by an orbital singlet state, whose orbital angular momentum projection along the NV^- axis vanishes. The ground states differ in the spin momentum projection m_S, which can take the values ±1 or zero. Accordingly, they are denoted by $^3A_{2\pm}$ or $^3A_{20}$. The six excited states with triplet character, which are involved in the zero-phonon transitions, are characterized by an orbital angular momentum quantum number of $|\mathbf{L}| = 1$. They are created by the excitation of an electron to either the e_x or e_y orbital; their orbital functions are composed of superpositions of the states $e_\pm = \mp a_1(e_x \pm ie_y)$ resulting in $|E_\pm\rangle = |a_1e_\pm - e_\pm a_1\rangle$, where the subindex $\pm$ denotes the orbital angular momentum projection $m_L = \pm1$ [27]. In combination with the spin states $|m_S\rangle = |\pm1\rangle$ and $|0\rangle$, the excited triplet states are given by $A_{1,2} = 1/\sqrt{2}(|E_-\rangle| + 1\rangle \mp |E_+\rangle| - 1\rangle)$, $E_{1,2} = 1/\sqrt{2}(|E_-\rangle| - 1\rangle \mp |E_+\rangle| + 1\rangle)$, and $E_{x,y} = |ae_{x,y} - e_{x,y}a\rangle|0\rangle$ with zero orbital angular momentum. In the presence of strain, spin-orbit, and spin-spin interactions at $B = 0$ T, the lowest-energy pair of states is $E_{1,2}$ followed by $E_{x,y}$ and $A_{1,2}$, for increasing energy [28].

By applying a sufficiently large external magnetic field $\mathbf{B}$, where the Zeeman energy exceeds the energy splitting due to strain, spin-orbit and/or spin-spin interactions, the states are split in accordance with their spin and orbital components of the Zeeman Hamiltonian:

$$H_Z = \mu_B g_S \mathbf{B}\cdot\mathbf{S} + \mu_B g_L \mathbf{B}\cdot\mathbf{L} + O(\mathbf{B}^2). \quad (3)$$

Here, g_S and g_L indicates the spin and orbital g-factor, respectively, μ_B is the Bohr magneton, and $\mathbf{S}$ is the spin operator. It is known that the spin g-factor is similar to that of a free electron, while the orbital g-factor is much smaller, taking values in the range of 0.1 [12,29,30]. The effect of a strong external magnetic field on the ordering of the excited and ground states of the NV^- center is schematically shown in Fig. 5(a). The states with spin momentum projection $+1$ are at highest energy, whereas those with $m_S = -1$ shift to lowest energy. For the excited states, each of the respective doublets is further split due to the orbital contribution. In this scheme the states are denoted by the orbital and spin momentum projections, following the notation $|m_L,m_S\rangle$. First, a ZPL describes a spin-conserving transition; the polarization of the emitted photon is determined by the orbital angular momentum projection only. Its change by $+1$ (-1) yields a σ^+-polarized (σ^--polarized) photon. Second, the ZPL energy does not contain the spin splitting energy. As far as one can presume an equal spin splitting for the ground and excited states and equal quadratic Zeeman Hamiltonian terms, the Zeeman splitting evaluated from the experimental PL data is given by

$$\Delta E_Z = \mu_B g_L B + \delta. \quad (4)$$

At high magnetic fields one can identify particularly the orbital contribution of the excited states to the zero-phonon transitions. This is also the case for the spin-conserving singlet-state transitions of the NV^- centers [see Fig. 5(a)].

For the NV^- centers measured in the (001), sample 1, and (111), sample 2, geometries, the Zeeman splittings of the 1.948- and 1.190-eV ZPLs practically coincide, as demonstrated by the linear fits according to Eq. (4) in Fig. 2. Their mean value is (9.5 ± 0.3) μeV/T, which corresponds to a positive orbital g-factor of $g_L = 0.164 \pm 0.006$. Hereby, it is important to underline that the energy of the σ^+-polarized ZPL of the SST exceeds that of the σ^--polarized line. As a consequence for the ordering of the levels, electrons relax from the $g_L\mu_B B$-split states of the $^1E'$ doublet radiatively to the $^1A_1$ level, as illustrated in Fig. 5(a). Since the Zeeman splitting of the ZPLs from the singlet-state transitions is similar to that of the ZPLs in which triplet states are involved, possible variations

in the ground- and excited-state spin splittings cannot account for the deviation of the evaluated g_L-factor from the previously reported g-factors of 0.1(0) [12,29,30]. The reason for the small g_L value could be drawn from the observation of the nonlinear magnetic field dependence of the absolute ZPL energies. In that case, the gradient of $E_{\mathrm{ZPL}}(B)$ is reduced at low magnetic fields so that the orbital g-factor appears smaller than that measured at high B fields. The previously reported orbital g-factors were mainly evaluated from electron-spin resonance experiments performed at hundreds of milliteslas. By comparison, a g_L-factor of 0.22 was obtained from the Zeeman splitting of the oppositely circular-polarized NV^- ZPLs at 150 T [13]. One has to note that an absolute error was not given to the latter value, although spectrally broad absorption lines were measured and their energies demonstrated fluctuations above approximately 30 T.

The quadratic evolution of the ZPL energies at intermediate magnetic field strengths may result from a mixing of excited states with nonzero orbital angular momentum. By analogy with that, such a field-induced mixing of orbital states also manifests itself as a quadratic variation of the hole Zeeman splitting in semiconductor quantum dots, which does not affect the circular polarization degree of the PL due to the undisturbed rotational symmetry of the respective Hamiltonian [31]. Only in sample 1 is the quadratic ZPL energy evolution present, while it is not the case for sample 2. One may claim that, for sample 1 with $\mathbf{B} \parallel (001)$, the transverse component of the magnetic field with respect to the NV^- symmetry (111) axis yields a mixing of the excited states with $L \neq 0$ [12]. Owing to the nonzero energy offset $\delta = 20\ \mu$eV at 0 T we moreover propose that strain and axial spin-spin interaction eliminate the excited-state mixing in sample 2 [28]. The offset, in turn, may result from the high NV center concentration, which is one order of magnitude larger than that in sample 1. Besides that, the magnetic field was directed along the crystal axes within a small error of $\pm 1^\circ$; therefore, a spatial misalignment can be neglected.

Furthermore, one observes four spectrally separated ZPLs in the different circular polarization configurations already at zero magnetic field in sample 2 and at high fields in sample 1. Of particular interest are the deviations between the energies of the ZPLs having the same circular polarization under optical excitation with opposite circular polarizations. This deviation depends about linearly on the magnetic field with a slope of $(1.1 \pm 0.2)\ \mu$eV/T, for both samples, while at 10 T it takes values of about 8 μeV (17 μeV), for sample 1 (2). It can be attributed to a difference in the spin splittings of the ground and excited states. In order to describe the experimental data, one has to assume that the spin splitting of the excited states (es) is larger than that of the ground states (gs), which is in contrast to Refs. [29,30]. In terms of the spin g-factor, it means that $g_{S,\mathrm{es}} = g_{S,\mathrm{gs}} + \Delta g$ with values of $\Delta g = 0.014$ and 0.029 in the (001), sample 1, and (111), sample 2, geometries, respectively. Additionally, one can conjecture that the excited states with positive (negative) m_S are predominantly excited by σ^+-polarized (σ^--polarized) light.

Circular polarization properties. As shown in Fig. 4(a), the circular polarization degree ρ_c^π significantly depends on the crystal orientation, which also alters the linear polarization degree of the NV^- ZPL [14]. Next to the angular dependence of ρ_c^π the symmetry axes of the NV^- center are depicted along the (001) direction. Due to crystallographic properties of the diamond crystal, the NV^- center appears in four orientations only, namely, along the (111), $(1\bar{1}\bar{1})$, $(\bar{1}1\bar{1})$, and $(\bar{1}\bar{1}1)$ directions [14,32]. When exciting along the (001) direction, one has to consider the two-dimensional (2D) projection about the (001) axis, which resembles a rectangular cross [compare Fig. 4(a)]. As one can see, ρ_c^π is maximal at about 135° and 315°. At these angles the polarization plane of the exciting laser light is parallel to the 2D projection of the NV^- centers oriented along the (111) and $(\bar{1}\bar{1}1)$ directions. Since the dipoles of the NV^- centers are oriented perpendicular to the symmetry axes of the center [33], such an excitation is not efficient [28]. However, in this geometry the polarization plane of the exciting laser is parallel to the dipole moments of the NV^- centers oriented along the $(\bar{1}1\bar{1})$ and $(1\bar{1}\bar{1})$ directions; hence, these centers can efficiently be excited. This leads to the conclusion that the emission of those centers is mainly σ^+ polarized. Vice versa, the NV^- centers, which are efficiently excited at a sample rotation of 45°, orientation along (111), and 225°, orientation along $(\bar{1}\bar{1}1)$, predominantly emit σ^--polarized ZPLs. At sample rotation angles of 0°, 90°, 180°, and 270° all NV^- centers are excited; thus, the emission does not have a preferable polarization and ρ_c^π is close to zero. It is worthwhile to mention that the NV^- centers, whose excitation leads to σ^+-polarized (σ^--polarized) ZPL emission, are inclined towards (away from) the optical z axis. ρ_c^σ, as shown in Figs. 4(b) and 4(c), has also an opposite sign compared to the data depicted in Fig. 3(b). Accordingly, the sign and values of both degrees of the circular polarization depend on the angular-dependent efficiency of the NV^- center excitation.

Moreover, the magnetic-field-dependent phase shift in the angular dependence of ρ_c^π is similar to that observed for the angle dependence of the linear polarization degree P_{lin} of the NV^- ZPL (see Ref. [14]). The phase shift may result from the magnetic torque of the external field acting on the magnetic moments of the NV^- center electrons [34,35], so that they tend to align in such a way that the total magnetic energy is minimized. Such a rotation of the magnetic moments could lead to a rotation of the angular dependence of the linear and circular polarization degrees, while it is more effective for the linear polarization degree, which demonstrated a phase shift of $\Delta\phi_0 = (27 \pm 1)^\circ$ [14]. Besides that, one may assume that the phase shift follows from a mixing of states with different magnetic moments under the application of a magnetic field specifically oriented with respect to the NV^- center symmetry axes.

Due to the switching of the sign of the circular polarization degree ρ_c^π through the rotation of the crystal, the slopes of the $\rho_c^\pi(B)$ dependencies could be compared to ρ_c^σ, which is measured at circularly polarized excitation. For the NV^- ensemble in sample 2, the slopes of the ρ_c^π and ρ_c^σ dependencies are in absolute terms 0.0021/T and 0.0035/T, respectively. By comparison, for the NV^- centers in sample 1, the corresponding slopes are 0.0053/T and 0.0014/T. In all cases, the dependencies tend to negative values for $B \gg 0$, which shows that the σ^--polarized excited states of the NV^- center are more likely to be occupied than the σ^+-polarized states, and vice versa for negative magnetic fields. It underlines the ordering of the level structure evaluated from the Zeeman splitting. The difference between the slopes of ρ_c^σ, for both samples, may be related to different level splittings and longitudinal

spin relaxation times due to differently strong spin-based interactions [36].

The decrease of the circular polarization degree at high temperatures is most likely due to electron-phonon coupling. As shown in Ref. [14], an acoustic-phonon-mediated coupling between the NV^- centers and adjacent lattice sites is mainly present in the crystals studied, since the ZPL energy and linewidth depend weakly on the temperature; a dynamic Jahn-Teller effect plays a minor role. In comparison to the linear polarization degree of 10% measured at room temperature, the circular polarization degree tends to zero. The small ρ_c^σ at high temperatures, see Fig. 4(b), can be attributed to the more efficient coupling of phonons to the excited levels with nonzero orbital and spin momenta. This effective spin-orbit coupling plays a dominant role for the states involved in the circularly polarized ZPLs. In that context, one has to note that the Zeeman splittings are smaller than the thermal energy $k_B T$ for the whole range of magnetic field strengths applied, even at $T = 6$ K. Therefore, it may make sense to study in the future the circular polarization degrees at temperatures below 1 K to exclude efficient contributions from electron-phonon interactions. In that case one may be able to observe a saturation of the circular polarization degree. In order to examine the impact of strain and crystal-field splittings on the circular polarization degree, one needs, for instance, to apply uniaxial stress in a controlled manner. The weak dependence of ρ_c^σ on the excitation energy, see Fig. 4(c), further highlights that the excitation selection rules are not lifted due to a nonresonant excitation through the phonon sidebands.

The practically zero circular polarization degree obtained for the singlet-state transitions of the NV^- centers, see Fig. 3(c), is probably due to a spin relaxation time being much shorter than the lifetime of the metastable $^1E'$ levels, i.e., an electron relaxation between the $^1E'$ levels is negligible so that a thermalization into the energetically lowest excited state does not occur.

B. Neutral nitrogen vacancy centers, NV^0

Let us now discuss the level structure of the NV^0 centers. The NV^0 consists of five electrons, from which three are distributed over the molecular orbitals a_1, e_x, and e_y. They form the ground state ^2E as well as the excited state ^2A, which is involved in the emission of the ZPL at about 2.16 eV. As depicted in Fig. 5(b), the excited state ^2A is a spin doublet, and due to the odd number of electrons it is split in two states with $+1/2$ and $-1/2$ spin-momentum projection numbers [8,9]. The ground state ^2E is additionally contributed by the orbital momentum of the e_x and e_y orbitals. One can propose two possible arrangements of the ground states.

In case (i), one should be able to distinguish at high magnetic fields between four states with respect to their different $m_S = \pm 1/2$ and $m_L = \pm 1$. Accordingly, one should observe left- and right-handed circularly polarized ZPLs separated in energy by the orbital Zeeman splitting. As shown in Fig. 2(c), the Zeeman splitting, for both circularly polarized excitations, is negligibly small; the average effective g-factor can be approximated to 0.017 ± 0.002. The weak magnetic-field-dependent splitting of the NV^0 ZPLs may hint at a small orbital Zeeman splitting of the ground states. In contrast to the NV^- center, for which the orbital contribution to the Zeeman splitting results solely in a splitting of the excited states, since the ground states have $m_L = 0$, the orbital Zeeman splitting of the NV^0 ground state would lead to an inverted Zeeman splitting of the ZPLs. This means that the σ^--polarized transition should be energetically higher than the σ^+-polarized ZPL and, as a consequence, the Zeeman splitting should be negative. This is, however, not observed. Moreover, ρ_c^σ is about zero and does not show any significant magnetic-field-dependent changes (slope of 0.0003/T). The high circular polarization degree ρ_c^π is instead due to the above-described directional and polarization-dependent excitation efficiency.

Therefore, we conclude that (ii) the ground state is composed of two states with compensated orbital contributions and opposite spin-1/2 momentum projections, as is sketched in Fig. 5(b). In such a scenario, the zero-phonon emission is not associated with a change of the orbital angular momentum projection and is therefore linearly polarized. A Zeeman splitting should be absent; the Zeeman splitting observed may stem from different spin Zeeman splittings of the ground and excited states, as in the case of the NV^- ensemble. This fine structure of the ground states reconciles more likely with the circular polarization degrees measured. Note that a contribution from the state $^4A_2$ with 3/2 angular momentum to the circular polarization features could not be outlined by our stationary PL experiments; time-resolved PL may indicate a possible involvement.

C. Neutral vacancies, V^0

The neutral single vacancy V^0, which is predominantly found in nonannealed diamonds with rather low nitrogen concentration [37], has four electrons located at the vacancy. Due to the T_d symmetry these electrons occupy the molecular orbitals a_1 and t_2 [10]. The configurations $a_1^1 t_2^2$ and $a_1^1 t_2^3$ give rise to a variety of states; here, we focus on the optically active transitions. The ground states ^1A and ^1E as well as the first-excited state $^1T_2$ are spin singlets. Note that, in contrast to the spin-degenerate states, like the spin quintet state $^5A_2$ which was studied with magnetic resonance methods [10], the optically active singlet states were rarely investigated. The ZPL at about 1.674 eV should stem from the transition between the $^1T_2$ excited to the ^1E ground state and the ZPL at about 1.666 eV should result from the transition between $^1T_2$ and the $^1A_1$ ground state [10,18].

Our results on the Zeeman splittings of the low- and high-energy V^0 ZPLs indicate an ordering of the ground states that is opposite to the above-mentioned one [see the level structure of the V^0 in Fig. 5(c)]. The high-energy ZPL of the neutral vacancy exhibits a positive splitting of 4.1 μeV/T; thus, the σ^+-polarized transition is highest in energy. The splitting describes the orbital Zeeman splitting of the $^1T_2$ states, to which we can attribute an orbital g-factor of $g_L = 0.071$. For the low-energy V^0 ZPL, the splitting amounts to -7.4 μeV/T. The electrons relax from the excited state $|0,0\rangle$ to the higher-lying $|+1,0\rangle$ and lower-lying $|-1,0\rangle$ ground states; thus, the observed negative splitting corresponds to a positive orbital g-factor of $g_L = 0.128$ for the ^1E states. It is interesting that the values of the g-factors differ from each other and from the orbital g-factor of the NV^- centers. Furthermore, our g-factor for the excited $^1T_2$ state is about four times larger than the value

of about 0.017, which was determined by magnetic circular dichroism measurements [20]. It was claimed that the orbital angular momentum of the $^1T_2$ states is strongly reduced by the dynamic Jahn-Teller effect [38]. In contrast to the ZPLs of the NV^- centers [14], the significant temperature-induced broadening of the V^0 ZPLs, see inset in Fig. 4(b), indicates a strong electron-phonon coupling, which may be attributed to a dynamic Jahn-Teller interaction [39]. One may assume that in our crystals the quenching of the orbital magnetic moment is less efficient due to more homogeneous vacancy environments or the strong magnetic field counteracts the bending distortion of the V^0 axes, which results from the dynamic Jahn-Teller effect. Besides that, if one assumes that the orbital g-factor is defined by the overlap integral of the vacancy envelope wave function with orbitals centered at the neighboring carbon ions, one can qualitatively state that g_L increases with the overlap integral or, respectively, with increasing average radius of the envelope function [40]. One may thus propose that the spatial distribution of the envelope function of the $^1T_2$ states is comparably narrow and is weakly affected by nonspherical distortions of the ion orbitals.

Moreover, we like to note that the V^0 ZPL energies change linearly with increasing magnetic field, and the ZPL energies, for oppositely circular-polarized excitation, coincide with each other (not shown here). The latter is obviously due to the fact that the ground and excited states are spin singlets. The former indicates the absence of a state mixing, although neither the ground nor the excited states are split at zero B field. It may arise from the large energetic separation of about 8 meV between the ^1E and ^1A states.

Finally, we take a look at the circular polarization properties of the V^0 ZPLs. ρ_c^π and ρ_c^σ for the high-energy ZPL demonstrate similar absolute values and similar absolute slopes of 0.0038/T and 0.0037/T, respectively. The small values of the circular polarization degrees mirror the orbital Zeeman splitting of the excited states defined by $g_L = 0.071$. The similarity of ρ_c^π with ρ_c^σ is due to the fact that, for the V^0, the linear polarization degree is small and practically isotropic against crystal rotations [14]. It could stem from the absence of a static dipole moment due to a symmetric electron distribution. For the low-energy V^0 ZPL, the circular polarization degree demonstrates an opposite slope as a function of the magnetic field strength. This is in agreement with the observed negative Zeeman splitting. Despite the larger orbital g-factor, $g_L(^1E) > g_L(^1T_2)$, the absolute values of ρ_c^π are small. Reasons for this weak circular polarization may be provided by future experiments involving pump-probe Faraday rotation which gain insight into the polarization dynamics.

V. CONCLUSION

Our detailed circular polarization-dependent magneto-optical studies provide insights into the fine structures of the NV^-, NV^0, and V^0 in diamond crystals. We evaluate the orbital g-factors for NV^- and V^0 ensembles by analyzing the Zeeman splittings of their ZPLs at magnetic fields of $-10\ \mathrm{T} \leqslant B \leqslant +10\ \mathrm{T}$. The circularly polarized ZPLs of the NV^- spin-singlet states result from $^1E' \rightarrow {}^1A_1$ transitions. The ground state ^1A of the neutral vacancy V^0 lies about 8 meV lower than the ^1E doublet. Furthermore, the energies of the NV^- spin-triplet ZPLs evolve quadratically with rising magnetic field strengths thus indicating a mixing of excited states with nonzero orbital angular momentum. The spin Zeeman splittings of the ground and excited NV^- triplet states deviate by about 1% from each other. Moreover, their circular polarization degree ρ_c^σ decreases significantly with rising temperature as a consequence of efficient spin-orbit coupling. The sign and value of ρ_c^σ can be changed strongly by rotating the diamond crystal around the (001) axis, while they are not affected by tuning the excitation energy from 2.22 down to 1.95 eV, i.e., close to the NV^- ZPL energy. Therefore, even with nonresonant excitation, enhanced circular polarization degrees can be achieved by choosing appropriate crystal orientations. Also, the studied ensembles of vacancies provide an enhanced statistical averaging of their optical properties which may be obscured by random variations of single vacancies.

ACKNOWLEDGMENT

We acknowledge financial support by the Deutsche Forschungsgemeinschaft in the frame of the ICRC TRR 160 (Projects No. A1 and No. B2).

[1] M. Hirose and P. Cappellaro, Coherent feedback control of a single qubit in diamond, Nature (London) **532**, 77 (2016).

[2] F. Dolde, H. Fedder, M. W. Doherty, T. Nöbauer, F. Rempp, G. Balasubramanian, T. Wolf, F. Reinhard, L. C. L. Hollenberg, F. Jelezko, and J. Wrachtrup, Electric-field sensing using single diamond spins, Nat. Phys. **7**, 459 (2011).

[3] B.-M. Chang, H.-H. Lin, L.-J. Su, W.-D. Lin, R.-J. Lin, Y.-K. Tzeng, R. T. Lee, Y. C. Lee, A. L. Yu, and H.-C. Chang, Highly fluorescent nanodiamonds protein-functionalized for cell labeling and targeting, Adv. Funct. Mater. **23**, 5737 (2013).

[4] N. Bar-Gill, L. M. Pham, A. Jarmola, D. Budker, and R. L. Walsworth, Solid-state electronic spin coherence time approaching one second, Nat. Commun. **4**, 1743 (2013).

[5] J. R. Maze, P. L. Stanwix, J. S. Hodges, S. Hong, J. M. Taylor, P. Cappellaro, L. Jiang, M. V. G. Dutt, E. Togan, A. S. Zibrov, A. Yacoby, R. L. Walsworth, and M. D. Lukin, Nanoscale magnetic sensing with an individual electronic spin in diamond, Nature (London) **455**, 644 (2008).

[6] L. P. McGuinness, Y. Yan, A. Stacey, D. A. Simpson, L. T. Hall, D. Maclaurin, S. Prawer, P. Mulvaney, J. Wrachtrup, F. Caruso, R. E. Scholten, and L. C. L. Hollenberg, Quantum measurement and orientation tracking of fluorescent nanodiamonds inside living cells, Nat. Nanotechnol. **6**, 358 (2011).

[7] M. W. Doherty, F. Dolde, H. Fedder, F. Jelezko, J. Wrachtrup, N. B. Manson, and L. C. L. Hollenberg, Theory of the ground state spin of the NV^- center in diamond, Phys. Rev. B **85**, 205203 (2012).

[8] S. Felton, A. M. Edmonds, M. E. Newton, P. M. Martineau, D. Fisher, and D. J. Twitchen, Electron paramagnetic resonance studies of the neutral nitrogen vacancy in diamond, Phys. Rev. B **77**, 081201 (2008).

[9] A. Gali, Theory of the neutral nitrogen-vacancy center in diamond and its application to the realization of a qubit, Phys. Rev. B **79**, 235210 (2009).

[10] J. A. Wyk, O. D. Tucker, M. E. Newton, J. M. Baker, G. S. Woods, and P. Spear, Magnetic-resonance measurements on the $^5A_2$ excited state of the neutral vacancy in diamond, Phys. Rev. B **52**, 12657 (1995).

[11] L. J. Rogers, S. Armstrong, M. J. Sellars, and N. B. Manson, Infrared emission of the NV centre in diamond: Zeeman and uniaxial stress studies, New J. Phys. **10**, 103024 (2008).

[12] L. J. Rogers, R. L. McMurtrie, M. J. Sellars, and N. B. Manson, Time-averaging within the excited state of the nitrogen-vacancy centre in diamond, New J. Phys. **11**, 063007 (2009).

[13] H. Hanzawa, H. Nishikori, Y. Nisida, S. Sato, T. Nakashima, S. Sasaki, and N. Miura, Zeeman effect on the zero-phonon line of the NV center in synthetic diamond, Physica B **184**, 137 (1993).

[14] D. Braukmann, V. P. Popov, E. R. Glaser, T. A. Kennedy, M. Bayer, and J. Debus, Anisotropies in the linear polarization of vacancy photoluminescence in diamond induced by crystal rotations and strong magnetic fields, Phys. Rev. B **97**, 125426 (2018).

[15] M. W. Doherty, N. B. Manson, P. Delaney, F. Jelezko, J. Wrachtrup, and L. C. L. Hollenberg, The nitrogen-vacancy colour centre in diamond, Phys. Rep. **528**, 1 (2013).

[16] Y. Ma, M. Rohlfing, and A. Gali, Excited states of the negatively charged nitrogen-vacancy color center in diamond, Phys. Rev. B **81**, 041204(R) (2010).

[17] M. L. Goldman, A. Sipahigil, M. W. Doherty, N. Y. Yao, S. D. Bennett, M. Markham, D. J. Twitchen, N. B. Manson, A. Kubanek, and M. D. Lukin, Phonon-Induced Population Dynamics and Intersystem Crossing in Nitrogen-Vacancy Centers, Phys. Rev. Lett. **114**, 145502 (2015).

[18] C. D. Clark and J. Walker, The neutral vacancy in diamond, Proc. R. Soc. London A **334**, 241 (1973).

[19] C. D. Clark and C. A. Norris, Photoluminescence associated with the 1.673, 1.944 and 2.498 eV centres in diamond, J. Phys. C: Solid State Phys. **4**, 2223 (1971).

[20] I. N. Douglas and W. A. Runciman, The magnetic circular dichroism spectrum of the GR1 line in irradiated diamonds, J. Phys. C **10**, 2253 (1977).

[21] T. A. Kennedy, F. T. Charnock, J. S. Colton, J. E. Butler, R. C. Linares, and P. J. Doering, Single-qubit operations with the nitrogen-vacancy center in diamond, Phys. Stat. Sol. B **233**, 416 (2002).

[22] J. Debus, D. Dunker, V. F. Sapega, D. R. Yakovlev, G. Karczewski, T. Wojtowicz, J. Kossut, and M. Bayer, Spin-flip Raman scattering of the neutral and charged excitons confined in a CdTe/(Cd, Mg)Te quantum well, Phys. Rev. B **87**, 205316 (2013).

[23] D. H. Goldstein, *Polarized Light* (CRC Press, Boca Raton, FL, 2010).

[24] *Optical Properties of 2D Systems with Interacting Electrons*, Nato Science Series II: Mathematics, Physics and Chemistry Vol. 119, edited by W. J. Ossau and R. Suris (Springer, Berlin, 2003), pp. 235–237.

[25] Note that the intensity of the SST-related NV^- ZPL is enhanced by a factor of 15. The deviation between the intensities of the ZPLs related to the singlet- and triplet-state transitions is mainly due to the different quantum efficiencies of the InGaAs- and Si-CCD cameras.

[26] M. W. Doherty, N. B. Manson, P. Delaney, and L. C. L. Hollenberg, The negatively charged nitrogen-vacancy centre in diamond: The electronic solution, New J. Phys. **13**, 025019 (2010).

[27] J. R. Maze, A. Gali, E. Togan, Y. Chu, A. Trifonov, E. Kaxiras, and M. D. Lukin, Properties of nitrogen-vacancy centers in diamond: The group theoretic approach, New J. Phys. **13**, 025025 (2011).

[28] E. Togan, Y. Chu, A. S. Trifonov, L. Jiang, J. Maze, L. Childress, M. V. G. Dutt, A. S. Sorensen, P. R. Hemmer, A. S. Zibrov, and M. D. Lukin, Quantum entanglement between an optical photon and a solid-state spin qubit, Nature (London) **466**, 730 (2010).

[29] G. D. Fuchs, V. V. Dobrovitski, R. Hanson, A. Batra, C. D. Weis, T. Schenkel, and D. D. Awschalom, Excited-State Spectroscopy Using Single Spin Manipulation in Diamond, Phys. Rev. Lett. **101**, 117601 (2008).

[30] P. Neumann, R. Kolesov, V. Jacques, J. Beck, J. Tisler, A. Batalov, L. Rogers, N. B. Manson, G. Balasubramanian, F. Jelezko, and J. Wrachtrup, Excited-state spectroscopy of single NV defects in diamond using optically detected magnetic resonance, New J. Phys. **11**, 013017 (2009).

[31] V. Jovanov, T. Eissfeller, S. Kapfinger, E. C. Clark, F. Klotz, M. Bichler, J. G. Keizer, P. M. Koenraad, M. S. Brandt, G. Abstreiter, and J. J. Finley, Highly nonlinear excitonic Zeeman spin splitting in composition-engineered artificial atoms, Phys. Rev. B **85**, 165433 (2012).

[32] N. Diep Lai, D. Zheng, F. Jelezko, F. Treussart, and J. Roch, Influence of a static magnetic field on the photoluminescence of an ensemble of nitrogen-vacancy color centers in a diamond single-crystal, Appl. Phys. Lett. **95**, 133101 (2009).

[33] R. J. Epstein, F. M. Mendoza, Y. K. Kato, and D. D. Awschalom, Anisotropic interactions of a single spin and dark-spin spectroscopy in diamond, Nat. Phys. **1**, 94 (2005).

[34] S. C. Rand, *Lectures on Light: Nonlinear and Quantum Optics Using the Density Matrix* (Oxford University Press, Oxford, U.K., 2016), Chap. 7.4.

[35] K. K. Hansen, D. V. Fedorov, A. S. Jensen, and N. T. Zinner, Classical crystal formation of dipoles in two dimensions, Phys. Scr. **90**, 125002 (2015).

[36] A. Jarmola, V. M. Acosta, K. Jensen, S. Chemerisov, and D. Budker, Temperature- and Magnetic-Field-Dependent Longitudinal Spin Relaxation in Nitrogen-Vacancy Ensembles in Diamond, Phys. Rev. Lett. **108**, 197601 (2012).

[37] K. Iakoubovskiia, G. J. Adriaenssensa, N. N. Dogadkinb, and A. A. Shiryaev, Optical characterization of some irradiation-induced centers in diamond, Diamond Relat. Mater. **10**, 18 (2001).

[38] J. E. Lowther and A. M. Stoneham, Theoretical implications of the stress and magnetic field splitting of the GR1 line in diamond, J. Phys. C **11**, 2165 (1978).

[39] J. C. A. Prentice, B. Monserrat, and R. J. Needs, First-principles study of the dynamic Jahn-Teller distortion of the neutral vacancy in diamond, Phys. Rev. B **95**, 014108 (2017).

[40] M. Thuau and J. Margerie, A theoretical calculation of the orbital g-factor of the excited state of F-centres in alkali halides, Phys. Stat. Sol. B **47**, 271 (1971).